Jurnal Kejuruteraan 33(2) 2021: 317-328
https://doi.org/10.17576/jkukm-2021-33(2)-16

Accurate Path-Loss Estimation for Wireless Cellular Networks

Ibrahim M M Mohamed
Electrical and Electronic Department, Faculty of Engineering, Omar Al-Mukhtar University, Al-Beida, Libya

**Corresponding author: engibrahim_2007@yahoo.com*

Received 27 April 2020, Received in revised form 19 September 2020
Accepted 10 October 2020, Available online 30 May 2021

ABSTRACT

In addition to its rule in achieving acceptable system performance, accurate path-loss estimation leads to realize a simple and precise estimation of cellular networks financial feasibility. In other words, in cellular networks, while accurate path-loss estimation helps to achieve a reasonable cost, inaccurate path-loss estimation could either lead to reduce the cost but degrade the performance, or improve the performance but increase the cost. Thus accurate path loss estimation becomes a very crucial and desirable goal. To this end, different models were introduced in the literature for achieving the aforementioned goal; however, each model sought to be a valid choice in a specific environment. Therefore, our main objective in this paper was to provide an insight to the cellular network designers to simplify the decision-making process. A number of widely used path-loss estimation models that work in different environments, such as Free-space model, Two-ray model, Okumura/Hata model, COST 231 model, and Indoor model were reviewed and analyzed. This significantly would assist any cellular network designer to select an appropriate model according to its working environment, and thus realize the desirable accurate path-loss estimation. Matlab was used to perform this analysis. The analysis drove us to enter into implicit comparisons between the aforementioned models. Going through these comparisons, it is concluded that although an increase in the level of complexity is encountered when using models with large number of correction factors, more accurate path-loss estimation can be achieved.

Keywords: Cellular networks (CNs); Path-loss estimation models; Free space propagation model; Two-ray model; Okumura/Hata model; Cost 231 model; Indoor model

INTRODUCTION

One of the main objectives of cellular systems is to achieve high capacity (i.e., increase the number of user). This objective can be realized by creating a distinctive way that guarantees exploiting the limited frequency spectrum assigned to the cellular systems efficiently. The concept of frequency re-use in which a segment of specific frequency spectrum can be used several times is the key to achieve an efficient exploit of the assigned spectrum. In frequency re-use theory, each cell within a single cluster represents a replica of each of six adjacent and predetermined cells (co-channel cells) surrounding it. Each co-channel cell belongs to a neighboring cluster. Although a low-power transmitter is commonly employed in each cell, a sufficient distance should be determined for separating the co-channel cells to guarantee minimum interference. Although interference can also come from the second, third, and higher tires co-channel cells, such interference can be ignored as it often contributes by less than one percent (1 %) of the total interference (Jochen 2003). As a type of communication system, the performance of a cellular system is indicated by its signal-to-noise ratio SNR. While the term signal refers to the power of an intended carrier, the term noise represents the power produced at the receiver due to thermal effect plus unwanted but received powers produced by the co-channel cells. For acceptable performance, a cellular system should meet a specific value of SNR. I.e. the SNR required for acceptable performance may differ from system to another. For example, approximately, a minimum SNR value of 18 dB or 12 dB is specified for acceptable performance when advanced mobile phone system AMPS or global system for mobile communication GSM is considered, respectively (Goldsmith 2005). In cellular systems, a wireless channel is mainly characterized by its effects of dispersion and attenuation. While dispersion is analyzed to verify which sort of signal distortion encountered during propagation, attenuation is analyzed to estimate the path-loss. In a wireless channel, a signal might be attenuated due to different phenomena, such as reflection, diffraction, and scattering. Reflection occurs when a signal that is propagating in a medium passes to another medium with different properties. Attenuation in this case can be attributed to the fact that a part of the incident signal energy is either absorbed or propagated into the reflecting medium. Diffraction is defined as the deviation of a signal from its path. It occurs when a signal that is propagating in a medium passes into a shadow region created by an obstruction. Scattering is defined as the spreading of energy out of its intended path. It occurs when a signal hits an object whose size is much smaller than or on the order of the signal wavelength. While accurate path-loss estimation helps to realize an acceptable system performance and leads to achieve reasonable cost, inaccurate path-loss estimation would either lead to degrade the performance or increase the cost (Andrea Goldsmith, 2005). Figure 1 (a), (b), and (c) clarify the aforementioned situations in which the estimated path-loss is higher than the actual path-loss in (a), almost equal to the actual path-loss in (b), or lower than the actual path-loss in (c).

Different models were introduced in the literature for achieving accurate path-loss estimation (Yoo-Seung Song & Hyun-Kyun Choi. 2017; Divya Kurup et al. 2011; Haipeng et al. 2010; Mario Versaci et al. 2012; A. Bhuvaneshwari et al. 2016; Yun-Jie Xu & Wen-Bin Li. 2011).

They were initially developed based on the simplest line-of-sight model; also referred to as free space propagation model. Later, they were developed based on more complicated non-line-of sight path-loss models. In free space propagation model, no obstructions due to earth surface or other obstacles are encountered during propagation. Unlike free space model in which frequency and separation distance (distance between transmitter and receiver) are the only contributors for path-loss, further factors such as antennas height, buildings height, and streets width are included in the non-line-of sight models, which leads to achieve more accurate path-loss estimation. Path-loss models can be categorized according to the separation distance as either long-distance prediction models or short-distance prediction models. They are intended for cellular systems employing macro-cells, and micro-cells, respectively. Pico-cells (cells that cover part of a building and mainly span from 30 to 100 *m*) can be included in the short-distance prediction models.

Indoor prediction models were introduced to estimate the path-loss in this case. Figure 2 provides a diagrammatic categorization of the path-loss models.

PREVIOUS WORK AND CONTRIBUTION

Many research studies, related to the path-loss were introduced in the literature. Zaarour et all, proposed a method to estimate the path-loss exponent PLE based on the connectivity between sensors deployed in a determined area (Nour Zaarour et al. 2016). Vaishnavi et all presented a practical method for path loss exponent calculation using the Received Signal Strength Indicator RSSI method which led to a minimal error in the distance estimation. The method was modeled mathematically using log-distance path loss model (Vaishnavi et al. 2018). Minthorn et all presented a method to estimate the wireless device location in indoor 2D environment using the widely used log-distance path loss model and actual Received Signal Strength Indicator (RSSI) measurement. The method showed an average difference of 7.42% from the measurement, which is considered acceptable for location estimation in actual environment (Minthorn et al. 2018). Agarwal and Jagannatham developed a homogenous Poisson point process based framework to characterize the performance of distributed estimation in wireless sensor

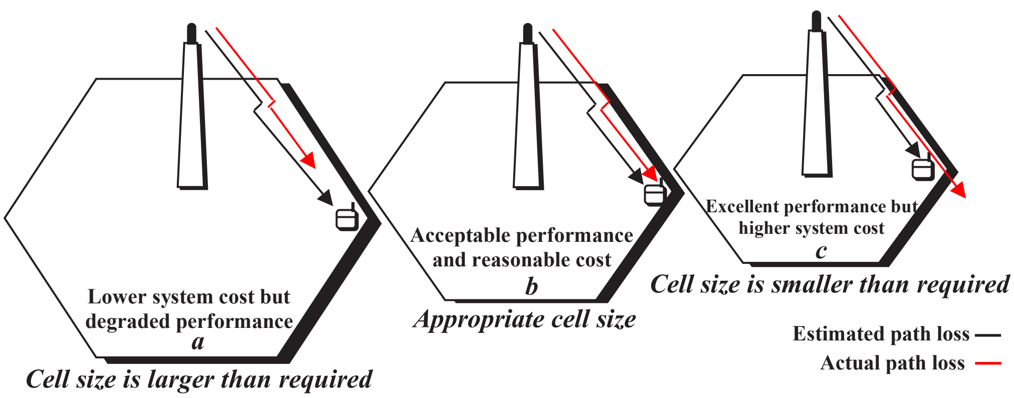

FIGURE 1. Effect of Accurate and Inaccurate Path-loss Estimation

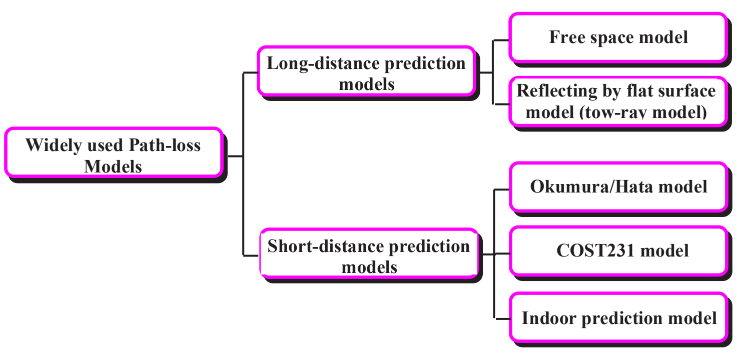

FIGURE 2. Widely used Path-loss Models

networks using a variety of scenarios in which a fading wireless channel was considered between the sensors and the Fusion Center (FC) (Abhishek et al. 2014). This paper provides an insight to the cellular network designers to simplify the decision-making process. A number of widely used path-loss estimation models that work in different environments, such as Free-space model, Two-ray model, Okumura/Hata model, COST 231 model, and Indoor model were reviewed and analyzed. This significantly assists any cellular network designer to select an appropriate model according to its working environment, and thus realize the desirable accurate path-loss estimation.

THEORETICAL BACKGROUND

In cellular networks, accurate path-loss estimation helps to precisely determine the number of cell sites required for providing coverage in a given area. Accurate path-loss estimation is highly recommended in the initial stages of cellular network design to precisely determine the number of cell sites required for providing coverage in a given area, which leads to achieve a simple estimation of financial feasibility. Additionally, accurate path-loss estimation leads to realize an acceptable system performance. Various path-loss estimation models were introduced in the literature; each of which is sought to be a valid choice in a specific environment and aiming to achieve accurate path-loss estimation. In this section, a review of theoretical background of few but widely used path-loss estimation models is provided.

LONG-DISTANCE PREDICTION MODELS

Free space model and two-ray model are the two widely used long-distance prediction models. In free space model, a line-of-sight propagation is assumed. i.e., no obstructions exist between transmitter and receiver albeit by the surface of earth. It is mostly applicable for wireless channels in which a transmission system such as microwave or satellite-to-satellite is employed. The path-loss in this case is referred to as free space path-loss (L_{Pfree}). Free space path-loss is given as (Vijay K. Garg, 2007).

$$L_{Pfree} = \left[\frac{4\pi d}{\lambda} \right]^2 \quad (1)$$

where d and λ represent the separation distance (i.e., distance between the transmitter and receiver) and wavelength, respectively. Given $\lambda = c/f$ yields

$$L_{Pfree} = \left[\frac{4\pi fd}{c} \right]^2 \quad (2)$$

where c and f represent the speed of light ($3\text{x}10^8$ m/sec) and frequency in hertz Hz, respectively. Substituting d in kilometer and f in megahertz, free space path-loss can be expressed in dB as

$$L_{Pfree[dB]} = 32.44 + 20Logf + 20Logd \quad (3)$$

It can be observed from (3) that duplication of frequency or distance would lead an increase in the path-loss by 6 dB. In the two-ray prediction model, multi-path propagation scenario is assumed in which a number of two propagation paths (direct propagation path and ground reflected propagation path) are considered. A part of the signal power is assumed to be received directly over the direct path (i.e., no obstructions between transmitter and receiver) whereas the rest is assumed to be received after being reflected by the ground surface). In this model, assumptions related to transmitter and receiver antenna heights (base station height h_b and mobile station height h_m), the angle between direct and reflected paths ($\Delta\alpha$), and reflecting surface are of significance for its validation. In theses assumptions, h_b and h_m are assumed to be much smaller than the separation distance d, $\Delta\alpha$ is assumed to be less than $\pi/8$, and reflecting surface is assumed to be flat. The model is valid for any distance d greater than $\bar{d}$ which is referred to as the critical distance and given as $\bar{d} = \frac{4h_b h_m}{\lambda}$. Figure 3 shows a schematic diagram of the two-ray model. The path-loss in this case is referred to as the two-ray path-loss ($L_{P2\text{-}ray}$).

Two-ray path-loss is given as (Vijay K. Garg, 2007) $L_{P2-ray} = \left[\frac{d^2}{h_b h_m} \right]^2$ which can be expressed in dB as

$$L_{P2-ray[dB]} = 20\log\left[\frac{d^2}{h_b h_m} \right] = 40\log d - 20\log(h_b h_m) \quad (4)$$

SHORT-DISTANCE PREDICTION MODELS

In this section, theoretical backgrounds related to the widely used short-distance prediction models, i.e., Okumura/Hata model, COST 231 model, and Indoor model are presented. While Okumura/Hata model and COST 231 model are recommended for path-loss estimation when micro-cells are used (separation distance might reach up to 50 km), Indoor model is the proper choice for path-loss estimation when pico-cells are used (separation distance might reach up to few hundred meters, i.e. probably inside a building).

OKUMURA/HATA MODEL

The Okumura/ Hata model was primarily developed for path-loss estimation in typical flat urban environment. Then it was improved to include path-loss estimation in the typical suburban and rural environments.

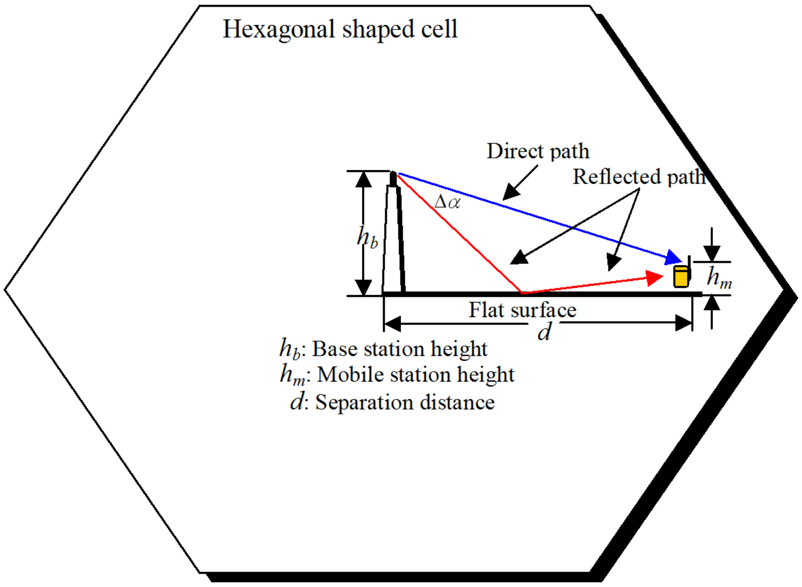

FIGURE 3. Two-ray Path-loss Model

A correction factor that is related to the mobile station antenna height was included in different forms according to the environment considered and frequency carrier used to achieve accurate path-loss estimation. The path-loss in *dB* according to Okumura/ Hata model for typical urban environment is given as (Garg 2007; Kazunori et al. 2014)

$$L_{50}(urban)_{[dB]} = 69.55 + 26.16\log fc + (44.9 - 6.55\log h)\log d - 13.82\log h - a(h_m) \quad (5)$$

Where fc is the carrier frequency in *MHz*, d is the separation distance between the mobile station and base station in *Km*, h_b and h_m are the base station and mobile station antennas height in meter, and $a(h_m)$ is correction factor that is related to the mobile station antenna height. $a(h_m)$is given in different forms according to the size of the intended area.

For large cities and at $fc \leq 200$ MHz, $a(h_m)$ is given as

$$a(h_m) = 8.29[\log(1.54h_m)]^2 - 11 \quad (6a)$$

For large cities and at $fc \leq 400$ MHz, $a(h_m)$ is given as

$$a(h_m) = 3.2[\log(11.75h_m)]^2 - 4.97 \quad (6b)$$

For small and medium-sized cities, $a(h_m)$ is given as

$$a(h_m) = [1.1\log(fc) - 0.7]h_m - [1.56\log(fc) - 0.8] \quad (6c)$$

The path-loss in *dB* according to Okumura/Hata model for the typical suburban environment is given as

$$L_{50}(suburban)_{[dB]} = L_{50}(urban) - 2\left[\left(\log\left(\frac{fc}{28}\right)^2\right) - 5.4\right] \quad (7)$$

The path-loss in *dB* according to Okumura/Hata model for the rural environment is given as

$$L_{50}(rural)_{[dB]} = L_{50}(urban) - 4.78(\log fc)^2 + 18.33\log fc - 40.94 \quad (8)$$

Table 1 provides the range of parameters for which Okumura/Hata model is valid (Vijay K. Garg, 2007).

COST 231 MODEL

The COST 231 model was developed based on empirical and deterministic approach for path-loss estimation in urban and suburban areas (L. M. Correia, 2009). It is resulted from the combination of Walfisch-Bertoni and Ikegami models (J.Walfisch & H. L. Bertoni. 1988; F. Ikegami et al. 1991). As compared with Okumura/Hata model, a number of additional correction factors, such as buildings' height and separation, streets' width, and orientation angle (the angle between the direction of propagation and street axis) have been added to the COST 231 model to achieve more accurate path-loss estimation. Figure 4 shows a schematic diagram of the COST 231 model. The path-loss in *dB* according to COST 231 model is given as (Vijay K. Garg, 2007; L. M. Correia, 2009)

TABLE 1. The range of parameters for which Okumura/Hata model is valid

	Minimum value	Maximum value
Carrier frequency *fc* (*MHz*)	150	2200
Base station height h_b (*m*)	30	200
Mobile station height h_m (*m*)	1	10
Separation distance *d* (*Km*)	1	20

$$L_{50[dB]} = L_f + L_{rts} + L_{ms} \tag{9}$$

In the case where $L_{rts} + L_{ms} \leq 0$, the path-loss in *dB* according to COST 231 model is given as

$$L_{50[dB]} = L_f \tag{10}$$

Where, L_f is the free space loss, L_{rts} is referred to as the roof-top-to-street diffraction and scatter, and L_{ms} is referred to as the multi-screen loss. Free space loss in *dB* can be expressed as in (3). The roof-top-to-street diffraction and scatter loss in *dB* is given as

$$L_{rts[dB]} = -16.9 - 10\log W + 10\log fc + 20\log \Delta h_m + L_o \tag{11}$$

W is the street width in meter, Δh_m is referred to as the difference between the average building height h_r and the mobile antenna height hm and given in meter as ($\Delta h_m = h_r - h_m$), and L_o is a correction factor, related to the orientation angle ϕ. L_o in *dB* can be given in different forms according to the orientation angle as

$$L_{o[dB]} = -10 + 0.354\varphi \quad \text{for} \quad 0 \leq \varphi \leq 35^o \tag{12a}$$

$$L_{o[dB]} = 2.5 + 0.075(\varphi - 35) \quad \text{for} \quad 35^o \leq \varphi \leq 55^o \tag{12b}$$

$$L_{o[dB]} = 4 - 0.114(\varphi - 55) \quad \text{for} \quad 55^o \leq \varphi \leq 90^o \tag{12c}$$

The multi-screen loss in *dB* is given as

$$L_{ms[dB]} = L_{bsh} + k_a + k_d Logd + k_f Logfc - 9Logb \tag{13}$$

where *b*, and *d* represent the distance between buildings along the radio path in meter, and separation between transmitter and receiver in *Km*, respectively.

L_{bsh} and k_d are correction factors that are related to the base station height and average building height. k_a is a correction factor that is related to the base station height, average building height, and separation distance. k_f is a correction factor that is related to the size of the city. L_{bsh} in *dB* can be given in different forms according to the base station height and average building height as

$$L_{bsh[dB]} = -18Log(11 + \Delta h_b) \quad \text{for} \quad h_b \geq h_r \tag{14a}$$

$$L_{bsh[dB]} = 0 \quad \text{for} \quad h_b < h_r \tag{14b}$$

Δh_b is referred to as the difference in meter between the base station height h_b and the average building height h_r and given as ($\Delta h_b = h_b - h_r$). k_a in *dB* can be given in different forms according to the base station height, average building height, and separation distance as

$$k_{a[dB]} = 54 \quad \text{for} \quad h_b > h_r \tag{15a}$$

$$k_{a[dB]} = 54 - 0.8h_b \quad for \quad d \geq 500m \quad \text{and} \quad h_b \leq h_r \tag{15b}$$

$$k_{a[dB]} = 54 - 0.8\Delta h_b (d/500) \quad for \quad d < 500\text{m} \quad \text{and} \quad h_b \leq h_r \tag{15c}$$

k_d is given in *dB* can be given in different forms according to the base station height and average building height as

$$k_{d[dB]} = 18 \quad \text{for} \quad h_b < h_r \tag{16a}$$

$$k_{d[dB]} = 18 - \left[\frac{15\Delta h_b}{\Delta h_m}\right] \quad \text{for} \quad h_b \geq h_r \tag{16b}$$

k_f in *dB* can be given in different forms according to the city size. For mid-sized cities, it is given as

$$k_{f[dB]} = 4 + 0.7\left[\frac{fc}{925} - 1\right] \tag{17a}$$

where as for metropolitan areas, it is given as

$$k_{f[dB]} = 4 + 1.5\left[\frac{fc}{925} - 1\right] \tag{17b}$$

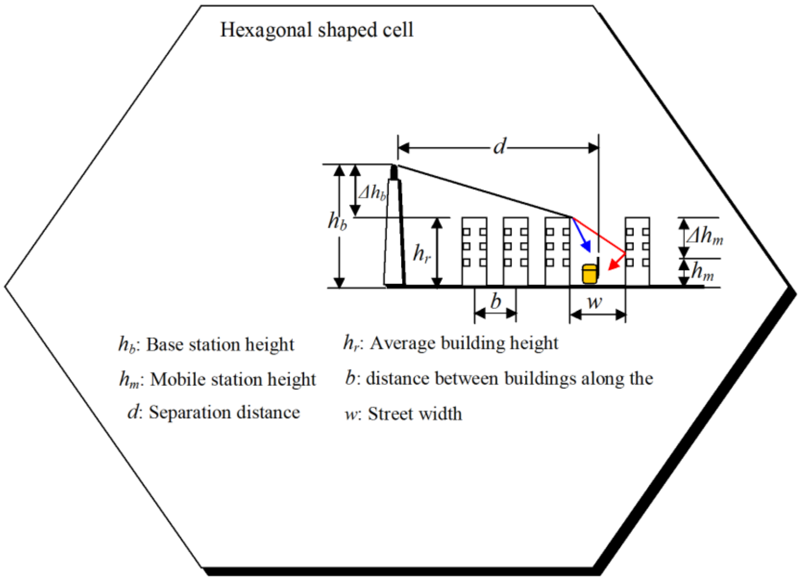

FIGURE 4. COST 231 Path-loss Model

Tables 2 and 3 provide the range of parameters for which the COST 231 model is valid and some default values that can be used in the COST 231 model (Garg 2007).

INDOOR PREDICTION MODEL

Indoor prediction model is recommended for path-loss estimation in the situation where cellular systems that employing Pico-cells are considered. A Pico-cell is defined as the cell specified for providing coverage in a small area, probably inside a building, i.e., could span up to 100 meters. It is mainly used in wireless systems operating in the indoor environment, such as wireless local area network WLAN and personal communication service PCS.

The path-loss in dB according to the Indoor prediction models is given as (Constantino et al. 1997)

$$L_{P[dB]} = \overline{L}_P(d_o) + 10\gamma Log d + L_f(n) + X_\sigma \tag{18}$$

Where $\overline{L}_P(d_o)$, γ, d, X_σ, and $L_f(n)$ are referred to as the path-loss at the first meter in *dB*, path-loss exponent, separation distance between transmitter and receiver in meter, shadowing effect in *dB*, and signal attenuation through *n* floors in *dB*, respectively. The values of $\overline{L}_P(d_o)$, γ, X_σ, and $L_f(n)$ are provided in Table 4 according to the indoor environment considered (Vijay K. Garg, 2007; Constantino et al. 1997). A value of signal attenuation per floor of either 10 *dB* or 16 *dB* can be used in the case where 900 *MHz* or 1.7 *GHz* is specified.

METHOD USED

As mentioned above, our goal is to provide a technical guide that would significantly help the cellular network designers speed up and simplify their decisions to use an appropriate path-loss model according to their work environment. This might involve us dealing with some complicated models that employ several correction factors when calculating the path-loss. To avoid this complexity in calculation and save the time, the method used in this paper was based on composing MATLAB computing programs that involve the loop mechanism. Figure 5 shows a flowchart sample that describes the sequence of program operation when Okumura/Hata model is used.

RESULTS AND DISCUSSIONS

This section is divided into two subsections. Results that cover path-loss estimations for long-distance prediction models were reviewed and analyzed in the first subsection whereas; results that cover path-loss estimations for short-distance prediction models were reviewed and analyzed in the second subsection. In both subsections, graphical representations of path-loss versus separation distance at different effective factors were provided.

In all cases, path-loss at any intended distance can be readily estimated by drawing a vertical line at that distance such that it intersects the path-loss versus distance curve and then draw a horizontal line from the intersection point; the value of path-loss in this case is the intersection point with the path-loss axis. Carrier frequencies of 900 *MHz*, 1800 *MHz*, and 2100 *MHz* were selected in the analysis. Matlab software was used for realizing the graphical representation.

PATH-LOSS ESTIMATIONS FOR LONG-DISTANCE PREDICTION MODELS

In this part of results, the path-loss is estimated by considering equations (3) and (5). Figure 6 shows the

TABLE 2. The range of parameters for which The COST 231 model is valid

	Minimum value	Maximum value
Carrier frequency *fc* in *MHz*	800	2000
Base station height h_b in *meter*	4	50
Mobile station height h_m in *meter*	1	3
Separating distance *d* in *kilometer*	0.02	5

TABLE 3. Some default values that can be used in the COST 231 model

Distance between building along radio path b	20 – 50 (m)
Street width W	b/2 (m)
Incident angle ϕrelative to the street	90º
Roof	3 m for pitched roof and 0 m for flat roof
Average building height hr	3(number of floors) + roof

TABLE 4. Values of indoor environments' parameters

	Indoor environment		
	Residential	Office	Commercial
$\overline{L}_P(d_o)_{[dB]}$	38	38	38
γ	2.8	3	2.2
$L_f(n)_{[dB]}$	4n	15+4(n-1)	6+3(n-1)
$X_{\sigma[dB]}$	8	10	10

graphical representation of (3). It represents the path-loss versus separation distance at different carrier frequencies, when free space model is used.

It is obviously seen from the graph that the path-loss starts to appear at a certain value of separation distance and continue to increase rapidly with a slight increase in the separation distance. However, it starts to increase steadily at higher values of separation distance. It is observed from the graph that the smallest value of path-loss is achieved at the lowest carrier frequency.

Figure 7 shows the graphical representation of (4). It represents the path-loss versus separation distance at different base station heights, when the two-ray model is used. It is obviously seen from the graph that the path-loss starts to appear at a certain value of separating distance in each case (the distance where the two-ray model is applicable [$d>>\overline{d}$]) and then continues to increase with the increase of the separation distance. However, an increase in the base station height leads to reduce the path-loss.

PATH-LOSS ESTIMATIONS FOR SHORT-DISTANCE PREDICTION MODELS

This part of results is divided into three sections. In the first section, path-loss is estimated using Okumura/Hata model, whereas in the second and third sections, path-loss is estimated using COST 231 model and Indoor model, respectively.

PATH-LOSS ESTIMATION USING OKUMURA/HATA MODEL

In this part of results, the path-loss is estimated using equations (5) to (8). The path-loss versus separation distance (1 *Km* to 20 *Km*) at different significant parameters, such as carrier frequency (900, 1800, and 2100 *MHz*), and base station height (20, 80, 140, and 200 *m*) were graphically represented. Figure 8 shows the graphical representation of equations (5), (6*a*) and (6*b*).

It represents the path-loss versus separation distance at different carrier frequencies, when the typical urban environment Okumura/Hata model for large cities is used. It is obviously seen from the graph that the path-loss starts to appear at a certain value of separation distance in which the model is valid (1 Km) and continue to increase with the increase in the separation distance. Figure 9 (a, b and c) shows the path-loss versus separation distance at different values of base station heights and carrier frequencies when typical urban environment Okumura/Hata model for large cities is used. The graph follows the same pattern as in Figure 8; however, an increase in the base station height leads to reduce the path-loss.

PATH-LOSS ESTIMATION USING COST 231 MODEL

In this part of results, the path-loss is estimated using equations (9) to (17b). We first provide graphical representations similar to those provided in the previous

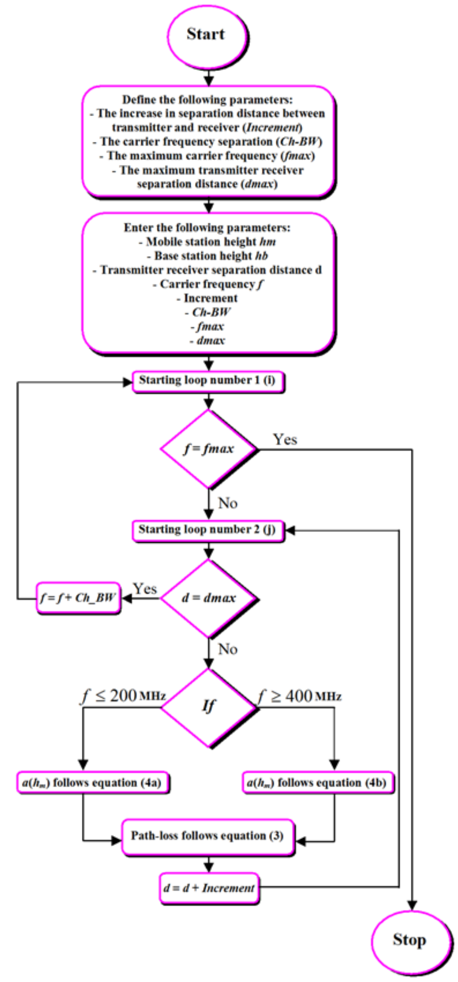

FIGURE 5. Sequence of Program Operation where Typical Urban Environment Okumura/Hata Model for Large Cities is considered

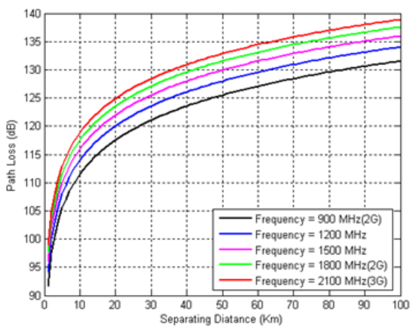

FIGURE 6. Path-loss vs Separating Distance at Different Carrier Frequencies: Free Space Model was Considered

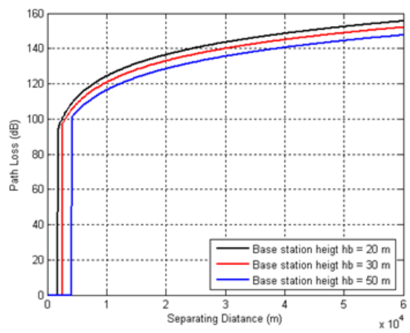

FIGURE 7. Path-loss vs Separating Distance at Different Base Station Heights: Two-ray Model Path-loss Model was Considered

sections, i.e., starting by draw the path-loss versus separation distance (1 to 50 Km) at different carrier frequencies (900, 1800, and 2100 MHz), and different base station heights (30, 40, and 50 m). Then, we provide extra graphical representations including further parameters that might affect the path-loss, such as the building heights (30, 60, 90, 120, and 150 m), road width (10, 15, 20, 25 m), and orientation angle (0o, 45o, and 90o). Figure 10 shows the path-loss versus separation distance at different carrier frequencies.

The graph follows the same pattern as in Figures 8 and 9; however, it shows higher path-loss values. For example, a path-loss value of 183.1184 *dB* is estimated at 20 *Km* separation and 2100 *MHz*, when using typical urban environment Okumura/Hata model for large cities, whereas a higher path-loss value (195.7259 *dB*) is estimated at the

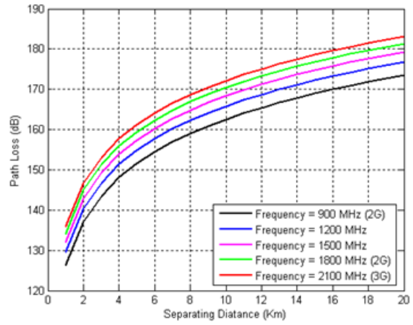

FIGURE 8. Path-loss vs Separating Distance at Different Carrier Frequencies: Typical Urban Environment Okumura/Hatta Model for Large Cities is Considered

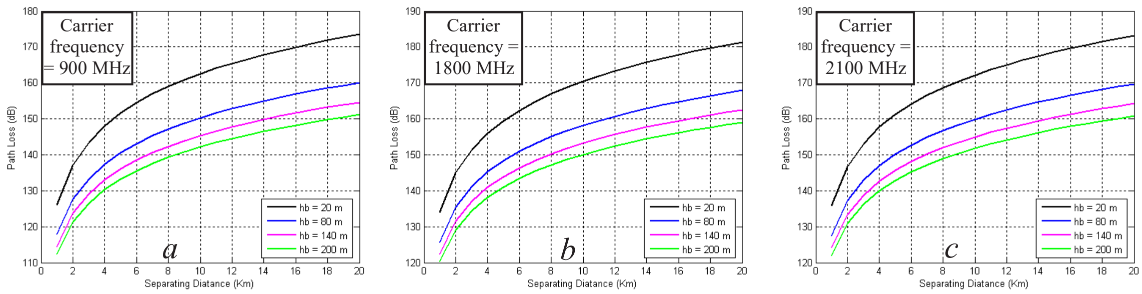

FIGURE 9. Path-loss vs Separating Distance at Different Base Station Heights: Okumura/Hatta model for Typical Urban Environment was Considered.

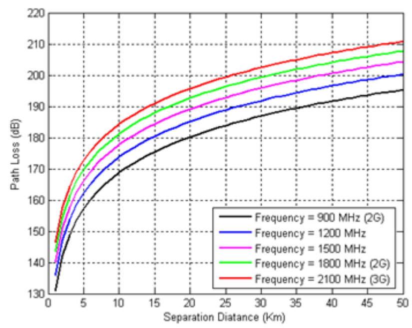

FIGURE 10. Path-loss vs Separating Distance at Different Carrier Frequencies: COST 231Model is Considered

same separation distance and frequency carrier when using COST 231 model.

Figure 11 (*a*, *b* and *c*) shows the path-loss versus separation distance at different values of base station heights and carrier frequencies when COST 231 model is used.

The graph follows the same pattern as in Figures 8, 9, and 10. The worth-mentioning point here is that identical path-loss values are estimated at the same separation distance (nearly 27 *km*) but at different base station heights (30 *m* and 50 *m*). Another worth-mentioning point is that the highest path-loss is always estimated when the base station height is 40 *m*. Figure 12 (*a*, *b* and *c*) shows the path-loss versus separation distance at different values of average building heights and carrier frequencies when COST 231 model is used. The graph follows the same pattern as in Figures 8, 9, 10, and 11. An increase in the average building height from 30 *m* to 60 *m* leads to a noticeable increase in the path-loss, whereas an increase in the average building height (from 60 to 90 *m*, from 90 to 120 *m*, or from 120 to 150 *m*) leads to gradual increase in the path-loss.

Figure 13 (*a*, *b* and *c*) shows the path-loss versus separation distance at different values of road widths and carrier frequencies when COST 231 model is used. Although the graph follows the same pattern as in Figures 8, 9, 10, 11, and 12, it reveals that there is an inverse proportional between the street width and the path-loss, i.e., as the width of the street increases, the path-loss decreases. Figure 14 (*a*, *b* and *c*) shows the path-loss versus separation distance at different values of orientation angles and carrier frequencies when COST 231 model is used. The graph follows the same pattern as in Figures 8, 9, 10, 11, 12, and 13. The observation here is that an increase in the orientation angle from 0^o to 45^o leads to a noticeable increase in the path-loss; however an

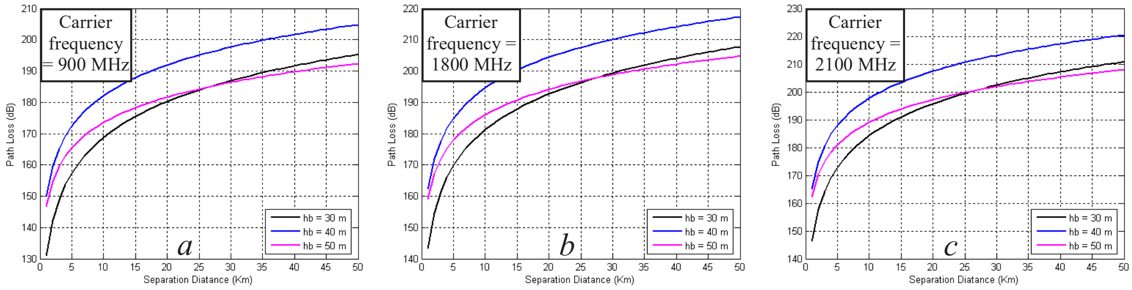

FIGURE 11. Path-loss versus separation distance at different base station heights: COST 231 model was considered.

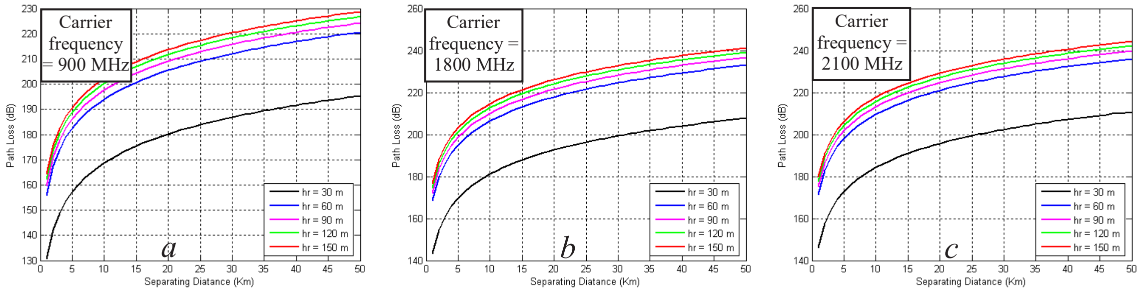

FIGURE 12. Path-loss vs Separation Distance at Different Building Heights: COST 231 Model was Considered.

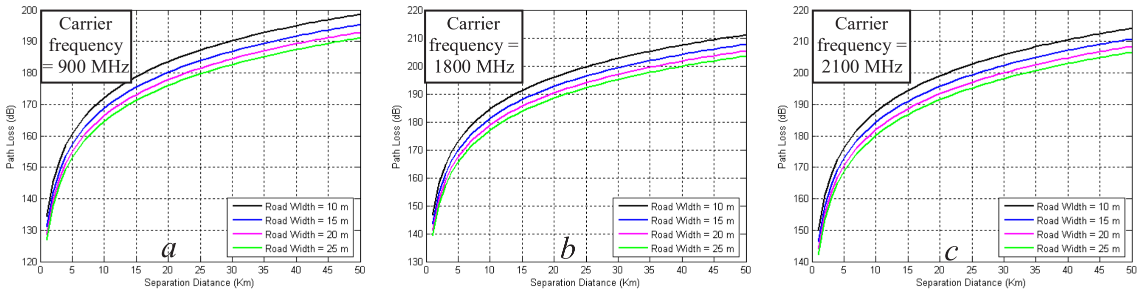

FIGURE 13. Path-loss vs Separation Distance at Different Road Widths: COST 231 Model was Considered.

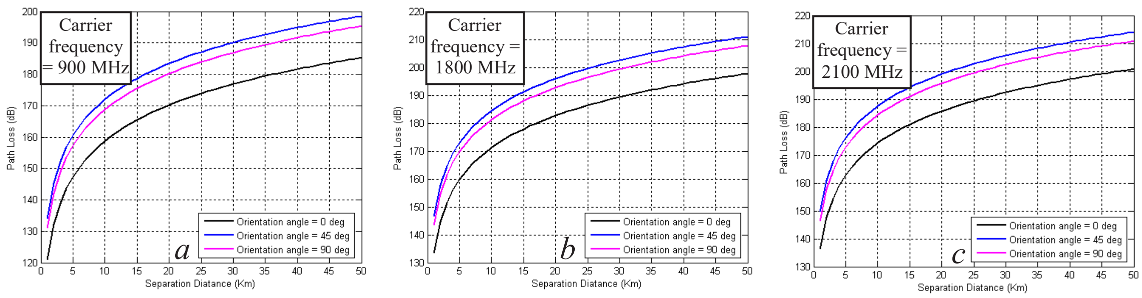

FIGURE 14. Path-loss vs Separation Distance at Different Orientation Angles: COST 231 Model was Considered.

increase in the orientation angle from 45^o to 90^o leads to reduce the path-loss.

PATH-LOSS ESTIMATION USING INDOOR PREDICTION MODEL

In this part of results, the path-loss is estimated using equation (18). Figure 15 shows the graphical representation of equation (18).

It represents the path-loss versus separation distance at different cases of indoor environment. In each case, the path-loss increases with the increase in the separation distance. A separation range lies between 30 to 100 *m* was used in the analysis as it represents the separation distance over which the indoor model is valid. The lowest path-loss is estimated in the case in which the commercial indoor environment is used, whereas the highest path-loss is estimated in the case in which the office indoor environment is used.

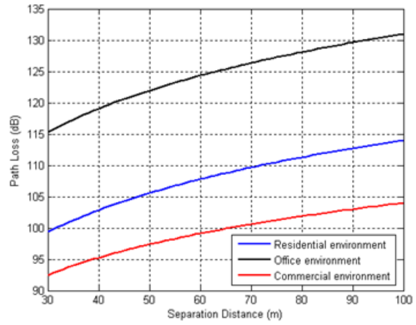

FIGURE 15. Path-loss vs Separation Distance: Different Cases of Indoor Environments are Considered

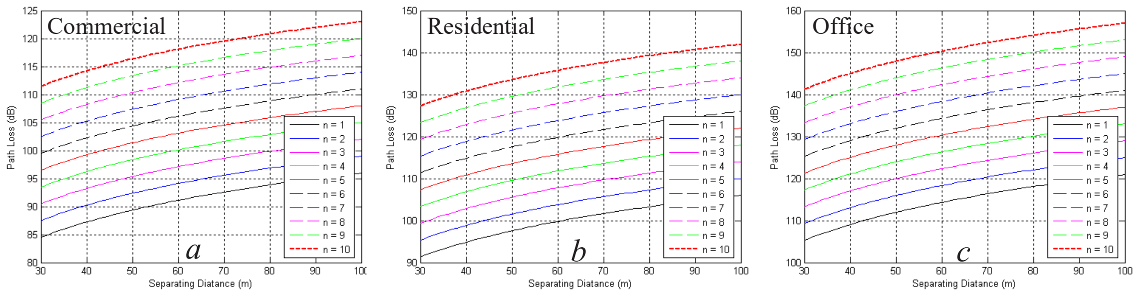

FIGURE 16. Path-loss vs Separation Distance at Different Number of Floors: (a): Commercial Indoor Environment, (b): Residential Indoor Environment, and (c): Office Indoor Environment.

Figure 16 shows path-loss versus separation distance at different number of floors when commercial, residential, and office indoor environments are considered. It is obviously seen that an increase in the separation distance leads to an increase in the path-loss. Furthermore, an increase in the number of floors leads to gradual increase in the path-loss.

CONCLUSIONS

In this paper, a number of widely used path-loss estimation models that work in different environments were reviewed and analyzed, which significantly would assist any cellular network designer to select an appropriate path-loss model according to its working environment. The study drove us to enter into implicit comparisons between the analyzed models.

Going through these comparisons, there were some significant observations that might be exploited advantageously. For example, results in Figures 7 and 9 confirmed that an increase in the base station height leads to reduce the path-loss. Although this observation can be exploited advantageously, i.e., it gives the opportunity to achieve a lower path-loss, it might affect the cost effectiveness of the cellular system. On other words, the base station height should be chosen such that it is comparable to the surrounding buildings. Result in Figure 11 confirmed that identical path-loss values are estimated at same separation distance (nearly 27 *km*) but at different base station heights (30 *m* and 50 *m*) when COST 231 model is used. This can be exploited advantageously, i.e., it gives the opportunity to reduce the cost by employing base stations with 30 *m* height instead of 50 *m* when the separation is less than or equal to 27 *Km*. However, base stations with 50 *m* height are recommended for use at further separations.

DECLARATION OF COMPETING INTEREST

None.

REFERENCES

Abhishek Agarwal., Aditya K., & Jagannatham. 2014. Distributed estimation in homogenous poisson wireless sensor networks. *IEEE Wireless Communications Letters* 3(1):90-93.

A. Bhuvaneshwari., R. Hemalatha., T. Satyasavithri. 2016. Semi Deterministic Hybrid model for Path Loss prediction improvement. *Proceeding of 2nd International Conference on Intelligent Computing, Communication & Convergence (ICCC-2016)* 336 – 344.

Andrea Goldsmith. 2005. *Wireless Communications*. Cambridge University Press.

Constantino Perez-Vegay., Jose Luis Garc´ıa Gy., & Jos´e Miguel L´opez Higueraz. 1997. A simple and efficient model for indoor path-loss prediction. *Meas. Sci. Technol* 8 (1997):1166–1173.

Divya Kurup., Maria Scarpello., Günter Vermeeren., Wout Joseph., Kristof Dhaenens., Fabrice Axisa., Luc Martens., Dries Vande Ginste., Hendrik Rogier., Jan Vanfleteren. 2011. In-body path loss models for implants in heterogeneous human tissues using implantable slot dipole conformal flexible antennas. *EURASIP Journal on Wireless Communications and Networking* Article ID 51

F. Ikegami., T. Takeuchi., & S.Yoshida. 1991. Theoretical prediction of mean field strength of urban mobile radio. *IEEE Trans. Antennas Propagat* 39(3):299–302.

Haipeng Ding., Zhengyuan Xu., Brian M. Sadler. 2010. A Path Loss Model for Non-Line-of-Sight Ultraviolet Multiple Scattering Channels. *EURASIP Journal on Wireless Communications and Networking* Article ID 598572

Schiller, J. H. 2003. *Mobile Communications*. Pearson Education Limited.

Walfisch, J. & Bertoni, H. L. 1988. A theoretical model of UHF propagation in urban environments. *IEEE Trans. Antennas Propagat* 36(12):1788–1796.

Kazunori Uchida, Naoto Hadano, Masafumi Takematsu & Junichi Honda. 2014. Propagation Estimation by Using Building Coverage and Floor Area Ratios Based on 1-Ray Model Combined with Okumura-Hata Model. *Proceeding of the 17th International Conference on Network-Based Information Systems* 555 – 560.

L. M. Correia. 2009. A View of the COST 231-Bertoni-Ikegami Mode. *Proceeding of the 3rd European Conference on Antennas and Propagation. EuCAP Berlin*.

Mario Versaci., Salvatore Calcagno., Fabio La Foresta., & Biagio Cammaroto. 2012. Ppath loss prediction using fuzzy inference system and ellipsoidal rules. *American Journal of Applied Sciences, Science Publication* 9(12):1940-1943

Minthorn Phunthawornwong, Eakkachai Pengwang & Rardchawadee Silapunt. 2018. Indoor Location Estimation of Wireless Devices Using the Log-Distance Path Loss Model, TENCON. *Proceeding of IEEE Region 10 Conference, South Korea* 28-31.

Nour Zaarour, Nahi Kandil, Sofiène Affes & Nadir Hakem. 2016. Path loss exponent estimation using connectivity information in wireless sensor network. *IEEE International Symposium on Antennas and Propagation (APSURSI), Fajardo, Puerto Rico*

Vaishnavi Dharmadhikari, Neha Pusalkar & Pradnya Ghare. 2018. Path Loss Exponent Estimation for Wireless Sensor Node Positioning: Practical Approach. *Proceeding of IEEE International Conference on Advanced Networks and Telecommunications Systems (ANTS), India* 6-19.

Garg, V. K. 2007. *Wireless Communications and Networking*. Elsevier.

Yoo-Seung Song & Hyun-Kyun Choi. 2017. Analysis of V2V broadcast performance limit for WAVE communication systems using two-ray path loss model. *ETRI Journal* 39(2):213-221

Yun-Jie Xu & Wen-Bin Li. 2011. Propagation path loss prediction model of multi-sensor network in forest. *Proceeding of Advanced in Control Engineering and Information Science Elsevier* 2206 – 2210.